Dalton Transactions

ROYAL SOCIETY OF CHEMISTRY

PERSPECTIVE

View Article Online
View Journal | View Issue

Cite this: *Dalton Trans.*, 2022, **51**, 4202

Recent advances in photorelease complexes for therapeutic applications

Andrew C. Benniston *[a] and Lingli Zeng [b]

Received 26th January 2022,
Accepted 16th February 2022

DOI: 10.1039/d2dt00254j

rsc.li/dalton

Photorelease complexes represent a class of agents for which UV-visible light triggers the expulsion of a specfic molecule that is intrinsically part of the inner coordination sphere or held in close proximity to the metal centre. The reaction does not occur in the ground-state complex and requires a photon, but an additional agent may be present that facilitates the release process. In this context, the perspective article covers recent papers from the past five years (2017–2021) on metal-based complexes containing ligands that are expelled under light activation. In addition, the examples primarily focus on ligands with potential biological activity and have specfic therapeutic applications. Some examples include NO, CO, Cl^-, peptides, pharmacophores and redox-active compounds.

1. Introduction

Light–matter interaction is critical for sustaining the vast majority of life on the planet Earth, providing the initial ignition to facilitate chemical and physical processes spanning from the ability to detect objects (*e.g.*, rhodopsin photoisomerization)[1] to mass flora production (*e.g.*, H_2O and CO_2 redox reactions).[2–4] The lessons learnt from the study of such natural processes provide the blueprint to design new compounds for which light is the decisive trigger to promote a physicochemical response. The general field of photodynamic therapy (PDT)[5] is one such example, designed for a variety of treatments such as tumour removal and requiring a specialised photoactive compound (PAC). The common feature is the active agent (*e.g.*, singlet oxygen, $^1O_2$) is produced by a secondary sphere interaction following light activation of the PAC.[6,7] Specifically, ground state oxygen (*i.e.*, $^3O_2$) must firstly diffuse to the PAC and undergo a triplet–triplet energy transfer process.[8,9] However, also within the broad envelope of PDT is the class of PACs for which light stimulation directly affects their core components to result in the ejection of a molecule.[10]

[a]*Chemistry-School of Natural & Environmental Sciences, Newcastle University, Newcastle upon Tyne, NE7 1RU, UK. E-mail: andrew.benniston@ncl.ac.uk*
[b]*Guangdong Provincial Key Laboratory of Malignant Tumor Epigenetics and Gene Regulation, Guangdong-Hong Kong Joint Laboratory for RNA Medicine, Medical Research Center, Sun Yat-Sen Memorial Hospital, Sun Yat-Sen University, Guangzhou 510120, China*

Andrew C. Benniston

Andy Benniston has spent a vast majority of his academic career at Newcastle University, after a spell at Glasgow University where he started as a lecturer. He is a professor in chemistry and has held several positions including Head of Chemistry, Deputy Head of School of Natural and Environmental Sciences and now the Associate Dean of Strategic Projects. His work has covered many different aspects including coordination chemistry of macrocycles, the photophysical properties of organic and inorganic compounds and artificial photosynthesis. He has published over 160 papers and co-written several review articles.

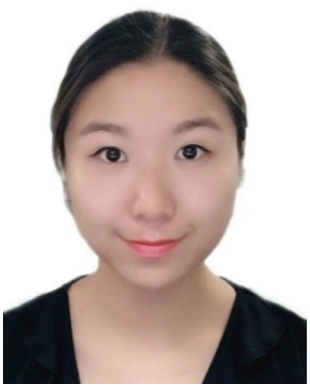

Lingli Zeng

Lingli Zeng is currently a postdoctoral researcher at the Sun Yat-sen University, Sun Yat-Sen Memorial Hospital. She obtained her PhD degree from Newcastle University in May 2020 under the supervision of Prof. Andrew Benniston. Her research interests include synthesis and applications of light-activated molecular systems, multimodel bioimaging, tumor diagnosis, drug delivery with nanosystems and the related disciplines. She has several publications in the fields of organic molecules, coordination compounds and nanomaterials for detection and tumor therapy.

The released molecule may have a direct therapeutic effect or play a key role in various physiological processes.[11] Since light can be highly focused and directed to a specific site the photorelease process can offer both spatial and temporal control for a therapy. There are of course downsides to the applicability of the method, since light does not penetrate far into dense objects, and light scattering and its absorption by other coloured compounds is difficult to avoid.[12]

Metal-based complexes dominate as examples of PACs especially those utilising polypyridyl ligands (*e.g.*, 2,2′-bipyridyl) coordinated to a ruthenium(II) metal centre.[13,14] One reason for their popularity stems from the rich and well understood basic photophysics for the complexes.[15] They are highly coloured because of light absorption associated with a metal-to-ligand charge-transfer (MLCT) band. The presence of the MLCT absorption band more importantly gives a suitable handle to photo-excite the complex and promote secondary processes. In this context, therefore, the concept of photorelease complexes is well established and they have been extensively studied for several years.[16] It is more recent that their application for therapeutics has grown in stature and forms the basis of this article. Examples are sampled from the past five years and several previously published reviews are highlighted for further detailed reading.[17]

2. Basic photophysics and photorelease mechanism

In order to appreciate the photorelease process, the basic photophysics of two archetypical complexes is highlighted; namely, $[Ru(bipy)_3]^{2+}$ (**Rubipy**) and $[Ru(terpy)_2]^{2+}$ (**Ruterpy**), where bipy = 2,2′-bipyridyl and terpy = 2,2′;6′,2″-terpyridine (Fig. 1). Even though both complexes are six coordinate and use similar donor groups, the precise geometry at the metal centre plays a major role in determining their photophysical properties. The poor bite angle for the terpy ligands in **Ruterpy** essentially means that the ligand-field splitting is weaker when compared to the **Rubipy** complex.[18] The importance of this effect becomes very clear when discussing the relative energies of electronic states within the two complexes (*vide infra*).

As mentioned previously the prominent ground-state absorption profile in the visible region for both complexes is associated with a ^{1}MLCT state, formed by electron migration from the ruthenium metal ion to an empty π* orbital on the polypyridyl ligand. The state can be written as Ru(III)-$L^{\bullet-}$, where L = bipy or terpy. It is worth noting that this representation helps explain why the excited complex can act as an oxidant (*i.e.*, Ru(III) + e^- → Ru(II) or a reductant ($L^{\bullet-}$ → L + e^-).[19,20] Extremely rapid intersystem crossing (<30 fs) results in efficient population of the triplet state (^{3}MLCT) from which processes for deactivation of the excited state originate (*e.g.*, luminescence).[21,22]

The secondary feature of the complexes is their d–d states, and the presence of the e_g* anti-bonding orbitals. The relative positioning of the ^{3}MLCT and the d–d states is especially critical in comprehending the lifetime of the ^{3}MLCT and the timescale available for a secondary process (Fig. 2). Room temperature emission from the ^{3}MLCT state for **Rubipy**[23] in fluid solution is readily observed but the same is not true for **Ruterpy**. Likewise the excited state lifetime for **Rubipy**[24] is in the microsecond region but only a few nanoseconds for **Ruterpy**.[25] The disparity in properties is explained by inspection of the **Ruterpy** potential energy surfaces and the closeness in energy of the ^{3}MLCT and d–d states (Fig. 2). Efficient electron cross-over into the d–d state results in rapid deactivation back to the ground state, facilitated by the favourable conical intersection (yellow line). The case for Rubipy is somewhat different since the ^{3}MLCT and d–d states are not so strongly coupled, requiring thermal population for deactivation. A point to note is the anti-bonding character of the d–d state and the fact that an electron will reside in it after the cross over process (*vide supra*). Hence, elongation of the Ru–N bond is expected,[26–28] leading to a weakening of the coordination bond. Despite what may appear to be a clear pathway for ligand loss both **Rubipy** and **Ruterpy** are stable in solution to light stimulation. There is a clear chelate effect, explained that even if one pyridine became detached the other anchoring ring would still hold the ligand in place.[29,30] A bond elongation process, by population of the anti-bonding metal-centred d-orbital, would appear to be more significant in a photorelease mechanism for monodentate ligands. The full ejection of a chelate after excitation

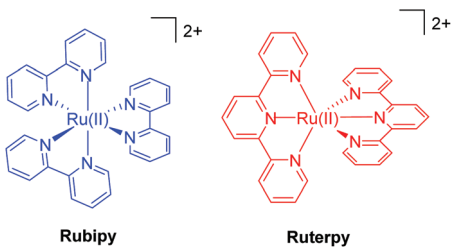

Fig. 1 Illustrations of the two archetypical complexes based on ruthenium(II) and the polypyridyl ligands 2,2′-bipyridyl (left) and 2,2′;6′,2″-terpyridine (right).

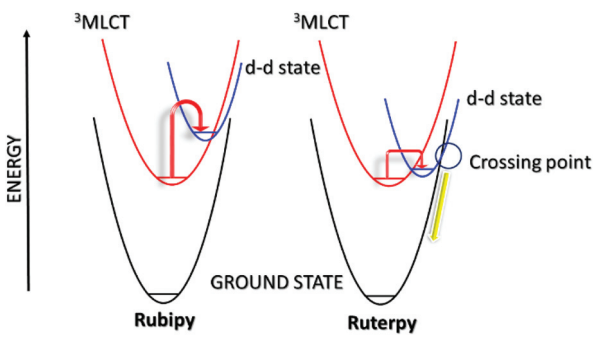

Fig. 2 Simplified potential energy surface diagrams for **Rubipy** (left) and **Ruterpy** (right). Note: the first-excited singlet ^{1}MLCT surface is omitted for clarity and the difference in energy between the potential energy surfaces are only qualitative.

may require a secondary agent, utilising the excited state redox properties of a complex. The excited state lifetime is more critical in this scenario since a bi-molecular reaction is now required.[31] The alternative to release a chelate is to introduce a steric effect, modify its electronic property or change the type of donor atom.[32]

Hopefully it is evident that exchange of a single terpy ligand in **Ruterpy** or one/two bipy ligand(s) in **Rubipy** for other donors, opens up the possibility for developing photorelease complexes. It is also reasonable to consider mixed bipy-terpy complexes or those where a pyridine is swapped for a different aromatic subunit. A further point to note is the capacity of the agent to be released to be an electron acceptor. In relation to Fig. 2 this introduces a further MLCT potential energy surface to consider with possible dissociative character and multiple surface crossing points. The following sections represent several different classes of photorelease agents based on the ruthenium(II) polypyridyl core. Other examples represent disparate types of complexes but still requiring light as the trigger.

3. Poly- and pyridine-based ligand dissociation

For most biological applications the photoreaction should ideally take place in aqueous solution. However, complexes invariably behave differently when dissolved in disparate solvents, and they will have influence on the ligand dissociation rate. To demonstrate this concept, Khnayzer and co-workers studied $[Ru(bipy)_2(dmphen)]^{2+}$ (dmphen = 2,9-dimethyl-1,10-phenanthroline) (**RU1a**). In acetonitrile the sterically constrained dmphen ligand is released much faster (half-life ~5 min) compared to water (half-life ~25 min). This observation was attributed to the better solubility of dmphen in acetonitrile.[33] Interestingly the complex was investigated against the ML-2 acute myeloid leukemia (AML) cancer cell line upon irradiation in water. The dmphen appears to be the cytotoxic agent rather than the $[Ru(bipy)_2(OH_2)]^{2+}$ ion produced during the dissociation process. Other work by Khnayzer and co-workers focused on the more constrained complex **RU1b**. The photophysics and photochemistry results showed that the complex can dissociate both bipyridine and the bathocuproine ligands.[34] However, not all the cytotoxic effects are caused by the ligand that is released from the light activation. For instance, to mimic the antitumor mechanism of cisplatin, Bonnet *et al.* demonstrated for the three ruthenium-based complexes $[Ru(bipy)_2(dmbpy)]^{2+}$ (**RU2a**), $[Ru(bipy)_2(mtmp)]^{2+}$ (**RU2b**), and $[Ru(Ph_2phen)_2(mtmp)]^{2+}$ (**RU2c**), it is the ruthenium bis-aqua photoproduct of $[Ru(Ph_2phen)_2(mtmp)]^{2+}$ instead of the ligand that kills the cancer cells.[35] Antitumor activity is always limited by the amount of a drug that accumulates in a cell. To improve cell uptake and nuclear accumulation levels, Zhou and co-workers obtained four pyridine-2-sulfonate (py-SO_3^-) ligand-based Ru(II) complexes (**RU3a–RU3d**). Under visible light the py-SO_3^- ligand dissociated and the remaining ruthenium bipyridine or phenanthroline precursor bound to DNA in what is termed photoactivated chemotherapy (PACT).[36] The mechanism of PACT is very classical in that the vacant coordination sites on ruthenium complex combine with base pairs of DNA and restrict its replication.

Periphery ligands with functional groups may also influence the properties of photorelease complexes. For example, Zhou and co-workers prepared pyridine-based ruthenium(II) complexes containing an additional fluorinated dppz (dipyridophenazine) ligand (**RU4**). The complexes undergo pyridine loss upon 470 nm irradiation coupled to DNA covalent binding. Compared to the parent complex, **RU4a**, the other complexes (**RU4b–RU4d**) displayed enhanced phototoxicity against tumor cell lines HeLa and SKOV-3 but diminished dark cytotoxicity, which is ideal for PACT. Meanwhile, in the normal cell line L-O2 the complexes exhibit less toxicity.[37] Follow up work tested the complexes for antibacterial activity against methicillin-resistant *Staphylococcus aureus* (MRSA), vancomycin-resistant Enterococcus (VRE), and *Escherichia coli* (*E. coli*). Compared to the parent un-fluorinated complex, the strong electronegativity of fluorine atom stabilizes the chemical structure, increases thermal stability and gives extra hydrogen bond interactions, expanding the application scope from antitumor to antibacterial.[38] A similar periphery ligand effect is demonstrated by the pyrene-based complex **RU5**, where the one pyridine of the terpy group is non-coordinating. Generally, a terpy ligand when fully coordinated is non photolabile. However, the uncoordinated pyrene-based terpy weakens the ligand-field and it is released under irradiation. The pyrene modification enables two-photon excited synergistic PDT and PACT activity, as well as "turn-on" fluorescence after ligand dissociation.[39]

The final example from Fig. 3 represents a complex (**RU6**) designed to photorelease a pharmacophore for application as

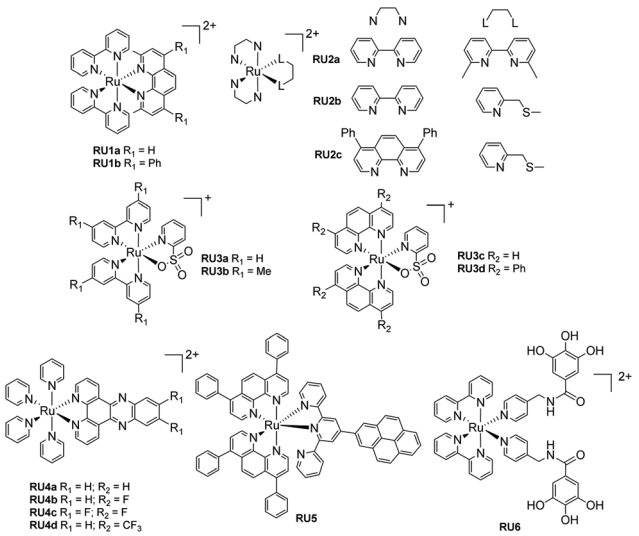

Fig. 3 Examples of ruthenium(II) polypyridyl complexes that undergo ligand loss upon irradiation in water.

a metalloenzyme inhibitor.[40] The key component is the gallic acid portion of **RU6** which is a recognized inhibitor of the N-terminal domain (PA_N) of the PA polymerase for the influenza virus. Basic experiments demonstrated that the pyridine–gallic acid conjugate was released from **RU6** following irradiation (λ_{irr} = 450 nm) in water. An enzymatic activity evaluation confirmed that the photoreleased conjugate was able to inhibit the PA_N endonuclease activity.

Generally, the photorelease of tridentate chelates is more difficult than bidentate chelates. The example **RU7** (Fig. 4) represents an interesting complex comprising a thioether-based terpy ligand (btap). White light irradiation of a solution of **RU7** in MeCN resulted in alterations in the absorption spectrum consistent with formation of the solvate complex and ejection of btap.[10]

4. Nitric oxide (NO) photorelease complexes

The discovery that nitric oxide ($NO^{\bullet}$) plays an important role in mammalian biological regulation and immunology, has aroused great interest in the chemistry and biochemistry of nitric oxide and its derivatives.[41] Also of interest are strategies for delivering $NO^{\bullet}$ on demand to biological targets.[42] In this context ruthenium(II) nitrosyl complexes $[(L)Ru(II)(NO^{+})]$, where L = any ligand(s), have been especially targeted since they often have low toxicity, good chemical stability, but are capable of releasing $NO^{\bullet}$ upon irradiation (eqn (1)).[43]

$$[(L)Ru(II)(NO^{+})] + \text{solvent} + h\nu \rightarrow [(L)Ru(III)(\text{solvent})] + NO^{\bullet} \quad (1)$$

It is worth noting the change in oxidation state of the ruthenium centre in the process of nitric oxide release (*i.e.*, +2 to +3). Interestingly DFT theoretical calculations (CASPT2) using *trans*-$[Ru(Cl)(NO)(py)_4]^{2+}$, where py = pyridine, supports that $NO^{\bullet}$ photorelease is a sequential two-photon process coupled with partial photoisomerization of the nitric oxide ligand.[44] This two-photon mechanism should certainly be considered for the ruthenium(II) polypyridyl nitrosyl examples illustrated in Fig. 5. The photorelease properties of complexes **RU8a** and **RU8b** were studied in DMSO by Malfant and co-workers,[45] both showing extreme sensitivity to traces of water and an equilibrium between the nitrosyl and nitro adduct. A similar set of complexes (**RU8c–RU8e**) had been previously studied by

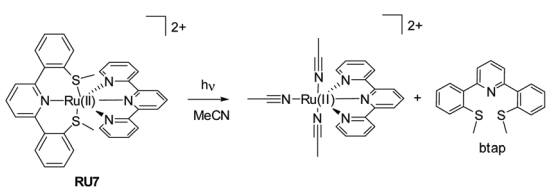

Fig. 4 Example of a mixed-ligand ruthenium(II) complex and the breakdown products formed under while light irradiation.

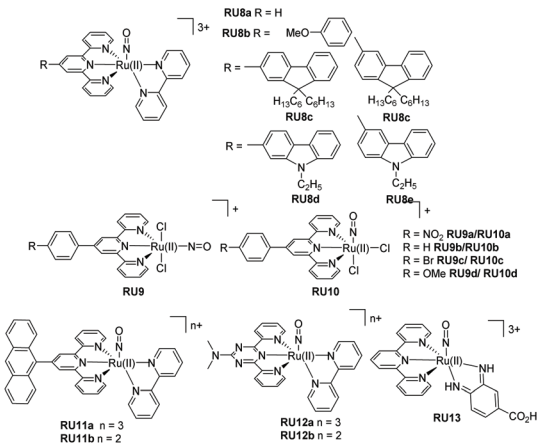

Fig. 5 Examples of NO photoreleasing agents based on ruthenium(II) terpyridine nitrosyl complexes.

the same group highlighting alterations in the $NO^{\bullet}$ releasing efficiency by swapping from fluorenyl to carbazole subunits.[46] The presence of the tertiary amine in the carbazole (**RU8d**, **RU8e**) introduced additional charge-transfer transitions toward the Ru-NO fragment. The observed enhancement of the two-photon absorption property for the complexes did not however manifest in an increase in the quantum yield for the $NO^{\bullet}$ release. This result is intriguing in the context of the theoretical calculations concept, demonstrating that the nitric oxide release mechanism may be very sensitive to electronic effects. The examples for the two series **RU9a–RU9d** and **RU10a–RU10d** were developed to investigate two effects on the photorelease of nitric oxide.[47] The first is the influence of the nature of the substituent on the 4′-positon of the terpy ligand, and the second is the change in the chloride position at the ruthenium metal centre (*i.e.*, *cis vs. trans*). The quantum yield (ϕ_{NO}) for the photorelease of $NO^{\bullet}$ was measured in MeCN for all the compounds. Across the series the ϕ_{NO} for the *cis* isomer was greater than the *trans* isomer. A simple explanation for the difference is the electron donating chloride *trans* to the $NO^{\bullet}$ facilitates its release. No correlation between ϕ_{NO} and the electron donating or withdrawing effect of the 4′-substituent was observed. One point to note is the same solvate photoproduct was produced for both the *cis* and *trans* isomers.

The final examples shown in Fig. 5 are from the group of Maji and co-workers.[16] In each case the tri-positive and di-positive complexes were prepared, the latter by chemical reduction of the bound nitric oxide ligand (*i.e.*, NO^{+} to $NO^{\bullet}$) The anthracene-based complexes **RU11a–RU11b** were specifically targeted for the treatment of prostate cancer. The rate of nitric oxide photorelease in MeCN for **RU11b** is *ca.* 4 fold greater than **RU11a**, under irradiation with a xenon light source (200 W). Presumably the change is related to a weakening of the Ru–N bond in the **RU11a** complex. The photo-cyctotoxicity of both complexes was determined against a VCaP human prostate cancer cell line. They demonstrated a reduction in VCaP cells after 6 hours of irradiation with white

light (400–700 nm). The complexes **RU12a** and **RU12b** contain the nitrogen-rich ligand *N*,*N*-dimethyl-4,6-di(pyridine-2-yl)-1,3,5-triazin-2-amine.[48] As noted in the previous examples the photorelease of nitric oxide is faster in the complex containing the reduced ligand; the difference in rates being *ca.* 5. For a very specific application the complex **RU13** was developed for treating skin diseases.[49] Specifically, the complex's penetration into skin was studied after the application of iontophoresis; the low level application of constant low-density electric current through an electrolyte and the skin. Compared to control experiments NO• release into skin was achieved using the complex.

The additional examples shown in Fig. 6 highlight bis-bidentate chelate ruthenium(II) complexes, with the two remaining coordination sites occupied by a NO^+ and another mono-dentate ligand. The complex **RU14** developed by Lopes *et al.*[50] was synthesised from its nitro precursor for testing if the complex was a vasodilator. Photorelease of NO• was confirmed by irradiation of an aqueous solutions of **RU14** (pH 2) at 365, 453 and 505 nm. A lower quantum yield of NO• release was noted when the long-wavelength light was employed. The two complexes **RU15a** and **RU15b**, again studied by the group of Lopes,[51] used the phenanthroline chelate and a thiocarbonyl subunit. As well as studying the nitric oxide release process further work studied their DNA cleaving properties in the presence and absence of blue light. Whereas complex **RU15a** promoted DNA damage both in the dark and the light, the same was not true for **RU15b** which required blue light activation. The complex **RU16** containing 2,2′-biquinoline (biq) is especially interesting since on its own poor NO• release was observed following white light irradiation in MeCN. However, significant enhancement occurred if the dichloride analogue $[Ru(II)(biq)_2Cl_2]$ was used as a co-sensitizer. It was hypothesised that a supramolecular dimer formed in solution, and from this species the NO• was released.[52] The more elaborate adduct **RU17** combines nitric oxide release with potential other free radical formation from the porphyrin group.[53]

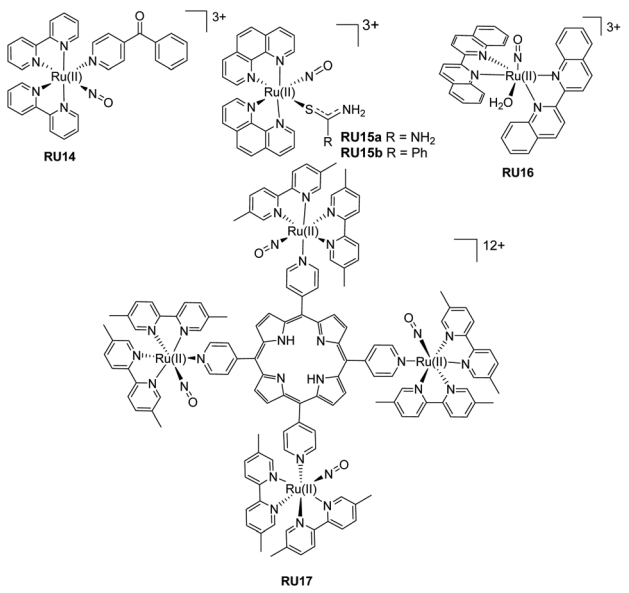

Fig. 6 Ruthenium(II) nitrosyl complexes based around bipyridine, biquinoline and phenanthroline ligands.

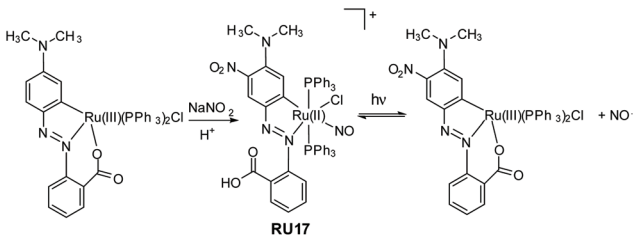

Fig. 7 Example of a ruthenium(II) cyclometalated nitrosyl complex prepared by Kumar and co-workers and the reversible loss and binding of nitric oxide under while light irradiation.

It is not exclusively necessary to construct nitric oxide photorelease complexes based around the ruthenium(II) polypyridyl core. The example shown in Fig. 7 is a disparate system developed by Kumar *et al.*; a cyclometalated derivative coupled to an azobenzene moiety.[54] The ruthenium(III) precursor when treated with sodium nitrite and acid produced the nitrosyl complex **RU17**, noting that the aromatic ring was also nitrated in the reaction. The complex when irradiated in DCM with white light resulted in loss of the NO•, but it is a reversible process as evidenced by spectroscopic measurements. The photoisomerization from *trans* to *cis* at the azobenzene unit is probably the driving force behind the NO• ejection process. The released nitric oxide could be trapped by reduced myoglobin in a phosphate buffer. Other measurements using fluorescent activated cell sorting analysis confirmed NO• release resulted in A549 human breast cancer cell death.

It should be noted that the photoinduced release of NO• molecules from pure organic components linked to a photosensitizer has also been explored by several groups. For instance, Thomsen *et al.* reported the room temperature release of NO from a cupferron *O*-alkylated with an anthracene derivative.[55] Nakagawa and his colleagues also conducted in-depth research in this direction using a hindered nitrobenzene derivative.[56]

5. Photorelease of other agents

The previous examples are classical as that much of the early worked on photodissociation used similar examples. This next section delves into complexes that release other molecules. It is broken down into two parts termed direct and indirect to represent the different characteristics of the photorelease process. In the direct reaction the agent to be released is directly attached to the metal centre as discussed previously, whereas in the indirect examples the agent is held in close proximity, but both still require a photon as the trigger. Other metal ions besides ruthenium are also considered.

5.1 Direct

Recognising that CO is isoelectronic with NO^+ it is not too surprising that studies have focused on its photorelease.[57] Carbon monoxide though poisonous in excess, is still one of the most important information molecules in the animal body and helps to regulate various physiological processes.[58] In addition, as a diagnostic reagent, CO plays a role in the treatment of inflammation and cell protection.[59] However, the real-time monitoring and study of CO in organisms are easily disturbed by the background. In the past decades, photoactive CO-releasing molecules (PhotoCORMs) have aroused scientists' interests because the CO molecule could be involved in immune and anti-inflammatory responses, as well as in vasorelaxation.[60]

A sample of recent PhotoCORMS are depicted in Fig. 8, again relying on the use of polypyridyl, triazole-based and thiazole-based compounds as the ancillary ligands. The complex **RU18** containing the triazamacrocycle was studied in depth by Slep and co-workers[61] using both steady-state and ultrafast transient absorption spectroscopic techniques. Steady-state photoinitiated CO release conducted in both water and MeCN showed that the solvento species was produced in both cases. This simple picture hides a more complicated process which was addressed by the ultrafast spectroscopic studies. The diagram shown in Fig. 9 represents the proposed species involved from the single occupied molecular orbitals (SOMOs) after excitation and their subsequent roles.

The complexes **RU19** and **RU20** represent examples based on the "Ru(bipy)$_2$CO" core, but where the final ligands in the coordination sphere are very different. The softer S donor is introduced in the second example. The irradiation of **RU19** in water with long-wavelength light (λ_{irr} = 453 nm) resulted in

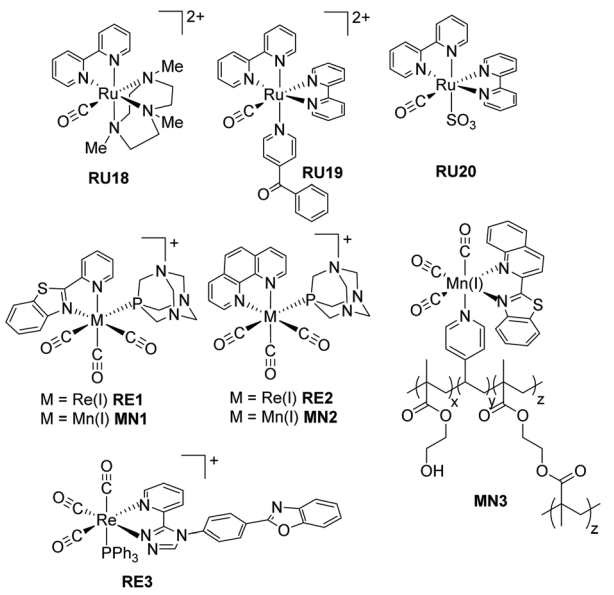

Fig. 8 Illustrations of PhotoCORMS based on ruthenium, rhenium and manganese complexes.

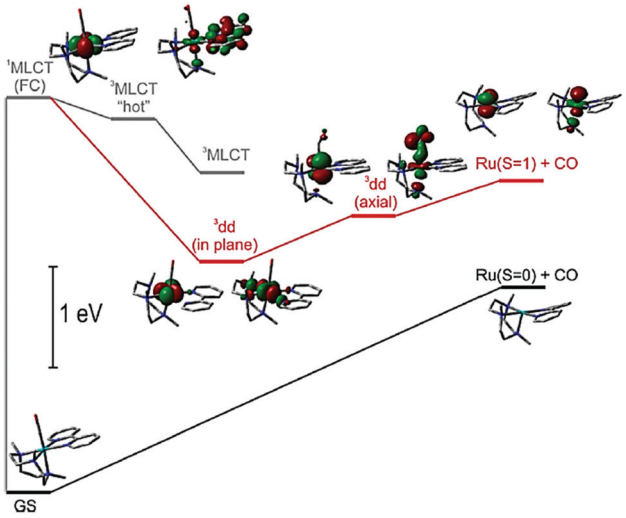

Fig. 9 Basic energy diagram representing the SOMOs of the states involved in the photophysics and photochemistry of **RU18**. Taken from ref. 61. Copyright permission © 2020 American Chemical Society.

selective loss of the benzoyl pyridine ligand and formation of the aqua complex $[Ru(bipy)_2(CO)H_2O]^{2+}$. A similar experiment performed using light of λ_{irr} = 365 nm firstly formed the same complex, which lost the CO ligand to finally generate $[Ru(bipy)_2(H_2O)_2]^{2+}$. The quantum yield ($\phi_{CO}$) for CO loss was found to be 0.041 ± 0.004.[62] It is worth noting that irradiation of **RU20** in water (λ_{irr} = 350 nm) resulted in only CO loss and a ϕ_{CO} = 0.301 ± 0.003.[63] These separate studies by two different groups would seem to suggest that secondary soft donors may enhance CO release in PhotoCORMS based around the "Ru(bipy)$_2$CO" core.

The remainder of the examples shown in Fig. 8 move way from ruthenium and focus on the other d^6 ions manganese(I) and rhenium(I). Three CO ligands are present and one of the other ancillary ligands is a polyaromatic. The complexes **RE1–RE2** and **MN1–MN2** were specifically designed to be water soluble by the addition of the 1,3,5-triaza-7-phosphasadamantane (PTA) to the coordination sphere.[64] A further aim was to produce photoCORMS that worked under low-power and broad-band visible light irradiation. Although **MN1** displayed no fluorescence in solution the release of CO under broad-band white light low-power (15 mW cm^{-2}) irradiation resulted in strong fluorescence centred at 400 nm. Interestingly the same was no seen for the complex **MN2**; the rate of CO loss was, in addition, slower under identical conditions. The loss of CO from the rhenium complexes **RE1** and **RE2** worked only under low power UV-A light (λ_{irr} = 360 nm, 5 mW cm^{-2}) and the dissociation rates for CO were comparable for the two complexes. Additional experiments focused on the luminescent complex **RE1** and demonstrated its cellular internalization in MDA-MB-231 (human breast cancer) cells. The manganese complexes **MN1** and **MN2** also exhibited dose-dependent eradication of MDA-MB-231 cells following irradiation and CO dissociation. The group of Mascharak developed the manga-

nese-based photoCORM concept by its incorporation into a polymer (**MN3**).[65] The polymer was used to release CO under low-power broadband visible light (<1 mW cm^{-2}) using a fibre optics technology approach. A fibre optical device was used to deliver CO to a suspension of human colorectal adenocarcinoma (HT-29) cells.

The final complex **RE3** incorporates the extended ligand based around pyridinetriazole and phenylbenzoxazole, with a triphenylphosphine to aid in the CO dissociation process.[66] Irradiation of a solution of **RE3** in MeCN at λ_{irr} = 350 nm resulted in absorption alterations consistent with CO loss and formation of the solvento complex. A ^{1}H NMR study coupled to a mass spectrometry experiment confirmed the loss of only one CO during the photolysis. The relatively strong emission observed from **RE3** diminished as the single CO was replaced by MeCN, consistent with previous findings on similar complexes. One drawback of **RE3** is its poor solubility in water and its self-aggregation.

5.2 Indirect

A series of fine examples of indirect release agents was designed and produced by Meyer and co-workers,[67] based on a supramolecular halide photorelease concept (Fig. 10). The early work by the group focused on **RU21** and **RU22**, noting that the halide binding site was kept constant but the electron donating/withdrawing effect at the two bipy ligands was changed. The design element behind this was to alter the direction of the excited state dipole moment. For complex **RU21** the MLCT dipole would point toward the halide but for **RU22** it would be directed away. The ground state binding constant towards chloride for both complexes in DCM was found to be *ca.* 4 × 10^6 M^{-1}. ^{1}H NMR experiments were consistent with the chloride binding to the R_2 side chains, rather than it sitting randomly in the second coordination sphere. Light excitation of **RU21** was shown to eject the chloride out the supramolecular cage. The binding constant was lowered by a factor of 20 in the excited state, meaning that around 45% of the chloride dissociated. In contrast, light excitation of **RU22** resulted in a 45 fold increase in the excited state binding constant. The ejection of the chloride can be rationalized in terms of a coulombic repulsion concept. The electron in the MLCT state for **RU21** will sit exclusively on the bipy containing the amide binding sites, and the repulsive electrostatic ion–ion repulsion essentially pushes out the chloride. Follow up work by the same group further studied the halide photorelease concept using **RU23** to **RU27** with chloride and bromide.[67,68]

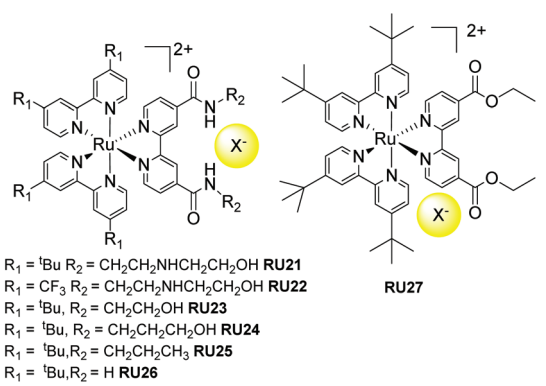

Fig. 10 Chloride photorelease complexes based on secondary supramolecular interactions with the amide functionalised bipy ligand.

6. Miscellaneous examples

In this section other direct photorelease complexes are noted that lack the presence of extended polyaromatic ligands at the metal centre. The use of the "Fe_2S_2" core is also discussed which is a disparate feature for NO$^\bullet$ release agents (Fig. 11). In addition, an illustration of light controlled release of therapeutic proteins from a cobalamin-based conjugate is considered in the context of protein therapeutics (Fig. 12). The ruthenium(II) nitrosulphito complex **RU27** is an interesting example produced by the reaction of *trans*-[$Ru(NH_3)_4$(isn)NO], where isn = isonicotinimide, with sulfite.[69] Previous to the work by Roveda and co-workers only four other similar complexes were known and their photochemistry was unexplored. The irradiation of **RU27** in phosphate buffered water (λ_{irr} = 355/410 nm) resulted in loss of the N(O)SO_3^- anion, which further decomposed to give NO$^\bullet$ and the sulfur trioxide anion radical ($SO_3^{\bullet-}$). There was no indication from the photolysis

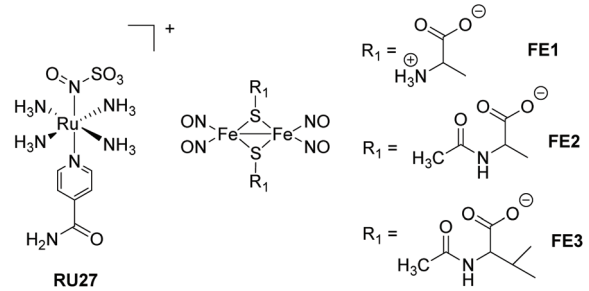

Fig. 11 Examples of other types of photorelease complexes.

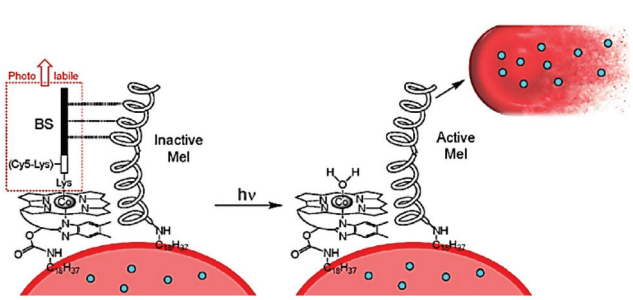

Fig. 12 A basic representation for the concept behind a photoactivated protein therapeutic, where ejection of the BS peptide unit activates the proximal protein to facilitate the loss of therapeutic proteins (blue dots) from the red blood cell (RBC). Taken from ref. 78. Copyright © 2020 American Chemical Society.

that a Ru^{3+} complex was formed, and so the final complex was assigned to $[Ru(NH_3)_4(H_2O)(isn)]^{2+}$. This dual release of two radicals may have further applications, especially considering the rich solution chemistry of the sulfite radical (eqn (2)–(4)).

$$SO_3^{\bullet -} + O_2 \rightarrow {}^{-}O_3SOO^{\bullet} \quad (2)$$

$${}^{-}O_3SOO^{\bullet} + SO_3^{2-} \rightarrow SO_4^{\bullet -} + SO_4^{2-} \quad (3)$$

$$SO_4^{\bullet -} + SO_3^{2-} \rightarrow SO_4^{2-} + SO_3^{\bullet -} \quad (4)$$

Roussin's red ester is a dimer nitrosyl-iron complex with the formula $[Fe(\mu\text{-}S)_2(NO)_4]^{2-}$, and has been extensively studied as a $NO^{\bullet}$ release agent.[70,71] Recent work by Lim *et al.* focused on the cysteine-derived complexes **FE1–FE3** which displayed excellent water solubility, suitable to complete an in-depth study into their photodissociation dynamics using femtosecond time-resolved infrared spectroscopy.[72] The thermal stability of the complexes **FE2** and **FE3** in water is around five times greater than the simple cysteine derivative **FE1**. Probing the excited state for **FE1–FE3** revealed that they released one $NO^{\bullet}$ to form $[Fe_2((\mu\text{-}RS)_2(NO)_3]$, or relaxed to the ground state without photodeligation *via* an electronically excited intermediate state. The loss of the single $NO^{\bullet}$ is extremely fast (<0.3 ps). Although $[Fe_2((\mu\text{-}RS)_2(NO)_3]$ combined with the solvent a small fraction also underwent geminate recombination with the $NO^{\bullet}$. The solvent complex was also shown to bimolecularly recombine with $NO^{\bullet}$ ($k = 1.3\text{–}1.6 \times 10^8\ M^{-1}\ s^{-1}$).

6.1 Amino acid and peptide release

The release of an amino acid or a peptide chain can be involved in regulating tumour cells apoptosis. For example, Rohrabaugh, Jr. *et al.* produced a new Ru(II) complex [Ru(terpy)(dppn)(Cbz-Leu-$NHCH_2CN$)]$^{2+}$, where dppn = benzo[*i*]dipyrido[3,2-*a*:2′,3′-*c*]phenazine to release the cathepsin K inhibitor Cbz-Leu-$NHCH_2CN$ ligand. And the resulting [Ru(terpy)(dppn)(OH_2)]$^{2+}$ was able to further generate $^1O_2$ for tumour cells apoptosis.[73] In the field of neurophysiology, scientists have made great efforts in modulating neural activities. Amino acids are also one of the most common neurotransmitters. Etchenique and co-workers developed the ruthenium-based caged 5-hydroxytryptamine (5HT) complex $[Ru(bipy)_2(PMe_3)(5HT)](PF_6)_2$ for modulating the excitability of mouse prefrontal principal neurons.[74] The similar derivative $[Ru(bipy)_2(PMe_3)Arg](PF_6)_2$, where Arg = arginine, could be photoactivated by blue or green light *via* one-photon excitation. The reduced L-arginine was able to elicit feeding response in the freshwater cnidarian *Hydra vulgaris*.[75]

Protein therapeutics is a growing area of research representing a class of drugs that are both selective and potent in their application.[76,77] However, deficiencies are their short circulatory lifetimes and side reactions at healthy tissue. One strategy is to keep the protein masked up to the point of action, and the use of red blood cells (RBCs) as carriers is a promising approach. The challenge is to control the release of proteins at the desired target. To this end the use of a photorelease process was demonstrated by the group of Lawrence as outlined in the simple picture of Fig. 12.[78] The concept is based on the well-established photochemistry of cobalamin (Cbl), in which the Co–C bond of methyl and adenosyl derivatives can be homolytically cleaved under light illumination (330–550 nm range). The working of the functionalized RBC of Fig. 12 relies on the release of the photolabile BS protein following white light illumination. The inactive melittin (Mel) protein is activated following this process, which then triggers the release of therapeutic proteins from the RBS. The successful application of photoresponsive thrombin loaded RBCs was demonstrated *in vivo* using FVB mice, noting that thrombin is capable of promoting clots in blood.

7. External agent assisted photorelease complexes

In the previous sections the function of the complexes only required input from light and no other agent was needed to facilitate the process. In this section the tenet of using the excited state-state redox chemistry to facilitate ligand loss is explored. The concept is not especially original[79] but the application for therapeutics is based on recognising that biological systems often contain oxidants and reductants.[80] It is proposed that the excited-state photochemistry could disturb their operating concentrations and result in loss of a ligand with detrimental/beneficial effects. Anthraquinone compounds fit the profile of possessing interesting therapeutic applications,[81,82] have a rich redox chemistry and can act as ligands to metal ions.[83] One problem arises from the low reduction potential for an anthraquinone which is manifested in a MLCT band of long-wavelength. At first this seems a positive feature for irradiation of a sample with low-energy white light, but has a negative effect of shortening the excited-state lifetime into the picosecond region.[84] Referring back to the picture of Fig. 1 the low-energy MLCT state introduced strongly couples to the ground state; non-radiative deactivation is highly efficient because of the energy-gap law.[85] The ultrashort excited lifetime would appear to preclude an effective bimolecular reaction with an oxidant/reductant from promoting efficient ligand dissociation. Despite this problem the two examples (**RU28–RU29**) shown in Fig. 13, with excited state

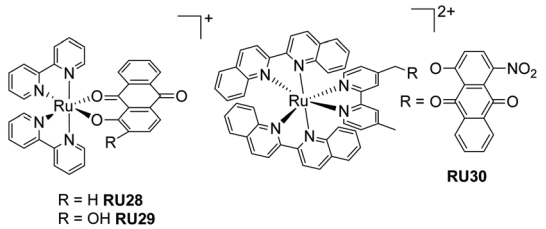

Fig. 13 Two anthraquinone-based ruthenium(II) complexes that decompose under light irradiation in the presence of hydrogen peroxide (left), and a ruthenium(II) bis-biquinoline complex appended with an anthraquinone.

lifetimes of only 5–7 ps, were shown to release the anthraquinone ligand in the presence of hydrogen peroxide.[86,87] The decomposition of **RU29** would appear to be promoted by an autocatalytic process, which helps explain why it can readily eject the anthraquinone. To date no biological experiments were carried out to ascertain if such complexes would have a therapeutic application. However, it is worth noting the triple functioning capability of the anthraquinone-based complex **RU30** as a PACT, photoredox catalyst and a PDT agent.[88] The ruthenium(III) centre and anthraquinones radical anion produced by **RU30** upon irradiation, and analogues to that created in **RU28** and **RU29**, will oxidize NADH/NADPH to form $O_2^{\bullet-}$ which is cytotoxic. The field of study for these type of complexes for therapeutic applications is clearly still at an early development stage.

8. Conclusions

This review has attempted to capture the recent advances made in photorelease complexes for therapeutic treatments. The application of complexes that eject CO or NO is certainly well established and there are numerous examples. More recent ultrafast time-resolved studies coupled to high-level DFT calculations have helped shed more light on the multifaceted nature of the dissociation process, and have pointed towards ways in which to improve future compounds. In comparison, the indirect release of an agent such as a halide or agent-assisted ligand photodissociation is still to be fully developed. Mitochondria targeting therapy is an area of research growing in popularity,[89,90] and may be the ideal target since they contain a plethora of redoxactive species. One could envisage disrupting the balance of reagents following the photoactivation of a drug.

Author contributions

This article was a joint project with equal contributions from the authors toward writing and literature surveys.

Conflicts of interest

There are no conflicts to declare.

Acknowledgements

We thank Newcastle University for financial support.

Notes and references

1 Y. Hontani, M. Broser, M. Luck, J. Weißenborn, M. Kloz, P. Hegemann and J. T. M. Kennis, *J. Am. Chem. Soc.*, 2020, **142**, 11464–11473.
2 S. K. Lee, M. Kondo, M. Okamura, T. Enomoto, G. Nakamura and S. Masaoka, *J. Am. Chem. Soc.*, 2018, **140**, 16899–16903.
3 M. A. Hoque, M. Gil-Sepulcre, A. de Aguirre, J. A. A. W. Elemans, D. Moonshiram, R. Matheu, Y. Shi, J. Benet-Buchholz, X. Sala, M. Malfois, E. Solano, J. Lim, A. Garzón-Manjón, C. Scheu, M. Lanza, F. Maseras, C. Gimbert-Suriñach and A. Llobet, *Nat. Chem.*, 2020, **12**, 1060–1066.
4 R. R. Rao, M. J. Kolb, L. Giordano, A. F. Pedersen, Y. Katayama, J. Hwang, A. Mehta, H. You, J. R. Lunger, H. Zhou, N. B. Halck, T. Vegge, I. Chorkendorff, I. E. L. Stephens and Y. Shao-Horn, *Nat. Catal.*, 2020, **3**, 516–525.
5 F. Heinemann, J. Karges and G. Gasser, *Acc. Chem. Res.*, 2017, **50**, 2727–2736.
6 P. Kumar, P. Singh, S. Saren, S. Pakira, S. Sivakumar and A. K. Patra, *Dalton Trans.*, 2021, **50**, 8196–8217.
7 N. Soliman, L. K. McKenzie, J. Karges, E. Bertrand, M. Tharaud, M. Jakubaszek, V. Guérineau, B. Goud, M. Hollenstein, G. Gasser and C. M. Thomas, *Chem. Sci.*, 2020, **11**, 2657–2663.
8 S. Cerfontaine, L. Troian-Gautier, S. A. M. Wehlin, F. Loiseau, E. Cauët and B. Elias, *Dalton Trans.*, 2020, **49**, 8096–8106.
9 V. Balzani, P. Ceroni, A. Credi and M. Venturi, *Coord. Chem. Rev.*, 2021, **433**, 213758.
10 A. Awada, F. Loiseau and D. Jouvenot, *Eur. J. Inorg. Chem.*, 2021, **2021**, 4539–4542.
11 H. Li, C. Xie, R. Lan, S. Zha, C.-F. Chan, W.-Y. Wong, K.-L. Ho, B. D. Chan, Y. Luo and J.-X. Zhang, *J. Med. Chem.*, 2017, **60**, 8923–8932.
12 R. Bensasson, C. Salet and V. Balzani, *J. Am. Chem. Soc.*, 1976, **98**, 3722–3724.
13 G.-B. Jiang, W.-Y. Zhang, M. He, Y.-Y. Gu, L. Bai, Y.-J. Wang, Q.-Y. Yi and F. Du, *J. Inorg. Biochem.*, 2020, **208**, 111104.
14 S. Li, G. Xu, Y. Zhu, J. Zhao and S. Gou, *Dalton Trans.*, 2020, **49**, 9454–9463.
15 J. G. Vos and J. M. Kelly, *Dalton Trans.*, 2006, 4869–4883.
16 B. Giri, T. Saini, S. Kumbhakar, K. K. Selvan, A. Muley, A. Misra and S. Maji, *Dalton Trans.*, 2020, **49**, 10772–10785.
17 J. Shum, P. K.-K. Leung and K. K.-W. Lo, *Inorg. Chem.*, 2019, **8**, 2231–2247.
18 M. T. Rupp, N. Shevchenko, G. S. Hanan and D. G. Kurth, *Coord. Chem. Rev.*, 2021, **446**, 214127.
19 E. Cuéllar, L. Pastor, G. García-Herbosa, J. Nganga, A. M. Angeles-Boza, A. Diez-Varga, T. Torroba, J. M. Martín-Alvarez, D. Miguel and F. Villafañe, *Inorg. Chem.*, 2020, **60**, 692–704.
20 D. Oyama, T. Kanno and T. Takase, *Dalton Trans.*, 2021, **50**, 7759–7767.
21 V. Vorobyev, D. S. Budkina and A. N. Tarnovsky, *J. Phys. Chem. Lett.*, 2020, **11**, 4639–4643.
22 A. Cannizzo, F. van Mourik, W. Gawelda, G. Zgrablic, C. Bressler and M. Chergui, *Angew. Chem.*, 2006, **118**, 3246–3248.

23 A. C. Bhasikuttan, M. Suzuki, S. Nakashima and T. Okada, *J. Am. Chem. Soc.*, 2002, **124**, 8398–8405.
24 T. P. Cheshire, M. K. Brennaman, P. G. Giokas, D. F. Zigler, A. M. Moran, J. M. Papanikolas, G. J. Meyer, T. J. Meyer and F. A. Houle, *J. Phys. Chem. B*, 2020, **124**, 5971–5985.
25 D. Luo, T. Zuo, J. Zheng, Z.-H. Long, X.-Z. Wang, Y.-L. Huang, X.-P. Zhou and D. Li, *Mater. Chem. Front.*, 2021, **5**, 2777–2782.
26 A. Soupart, F. Alary, J.-L. Heully, P. I. P. Elliott and I. M. Dixon, *Inorg. Chem.*, 2020, **59**, 14679–14695.
27 A. Soupart, F. Alary, J.-L. Heully, P. I. P. Elliott and I. M. Dixon, *Inorg. Chem.*, 2018, **57**, 3192–3196.
28 M. Asahara, H. Kurimoto, M. Nakamizu, S. Hattori and K. Shinozaki, *Phys. Chem. Chem. Phys.*, 2020, **22**, 6361–6369.
29 M. S. Meijer and S. Bonnet, *Inorg. Chem.*, 2019, **58**, 11689–11698.
30 M. Hirahara, H. Nakano, K. Uchida, R. Yamamoto and Y. Umemura, *Inorg. Chem.*, 2020, **59**, 11273–11286.
31 A. Soupart, F. Alary, J.-L. Heully, P. I. P. Elliott and I. M. Dixon, *Coord. Chem. Rev.*, 2020, **408**, 213184.
32 D. Lazić, A. Scheurer, D. Ćoćić, J. Milovanović, A. Arsenijević, B. Stojanović, N. Arsenijević, M. Milovanović and A. R. Simović, *Dalton Trans.*, 2021, **50**, 7686–7701.
33 D. F. Azar, H. Audi, S. Farhat, M. El-Sibai, R. J. Abi-Habib and R. S. Khnayzer, *Dalton Trans.*, 2017, **46**, 11529–11532.
34 S. Mehanna, N. Mansour, H. Audi, K. Bodman-Smith, M. A. Mroueh, R. I. Taleb, C. F. Daher and R. S. Khnayzer, *RSC Adv.*, 2019, **9**, 17254–17265.
35 J.-A. Cuello-Garibo, M. S. Meijer and S. Bonnet, *Chem. Commun.*, 2017, **53**, 6768–6771.
36 N. Tian, Y. Feng, W. Sun, J. Lu, S. Lu, Y. Yao, C. Li, X. Wang and Q. Zhou, *Dalton Trans.*, 2019, **48**, 6492–6500.
37 R. Boerhan, W. Sun, N. Tian, Y. Wang, J. Lu, C. Li, X. Cheng, X. Wang and Q. Zhou, *Dalton Trans.*, 2019, **48**, 12177–12185.
38 W. Sun, R. Boerhan, N. Tian, Y. Feng, J. Lu, X. Wang and Q. Zhou, *RSC Adv.*, 2020, **10**, 25364–25369.
39 Z. Jin, S. Qi, X. Guo, Y. Jian, Y. Hou, C. Li, X. Wang and Q. Zhou, *Chem. Commun.*, 2021, **57**, 3259–3262.
40 J. Karges, R. W. Stokes and S. M. Cohen, *Dalton Trans.*, 2021, **50**, 2757–2765.
41 A. A. Mikhailov, D. V. Khantakova, V. A. Nichiporenko, E. M. Glebov, V. P. Grivin, V. F. Plyusnin, V. V. Yanshole, D. V. Petrova, G. A. Kostin and I. R. Grin, *Metallomics*, 2019, **11**, 1999–2009.
42 B. Giri, S. Kumbhakar, K. K. Selvan, A. Muley and S. Maji, *Inorg. Chim. Acta*, 2020, **502**, 119360.
43 A. Enriquez-Cabrera, I. Sasaki, V. Bukhanko, M. Tassé, S. Mallet-Ladeira, P. G. Lacroix, R. M. Barba-Barba, G. Ramos-Ortiz, N. Farfán, Z. Voitenko and I. Malfant, *Eur. J. Inorg. Chem.*, 2017, **2017**, 1446–1456.
44 F. Talotta, L. González and M. Boggio-Pasqua, *Molecules*, 2020, **25**, 2613.
45 N. Marchenko, P. G. Lacroix, V. Bukhanko, M. Tasse, C. Duhayon, M. Boggio-Pasqua and I. Malfant, *Molecules*, 2020, **25**, 2205.
46 A. Enriquez-Cabrera, P. G. Lacroix, I. Sasaki, S. Mallet-Ladeira, N. Farfán, R. M. Barba-Barba, G. Ramos-Ortiz and I. Malfant, *Eur. J. Inorg. Chem.*, 2018, **2018**, 531–543.
47 S. Amabilino, M. Tasse, P. G. Lacroix, S. Mallet-Ladeira, V. Pimienta, J. Akl, I. Sasaki and I. Malfant, *New J. Chem.*, 2017, **41**, 7371–7383.
48 B. Giri, S. Kumbhakar, K. K. Selvan, A. Muley and S. Maji, *New J. Chem.*, 2020, **44**, 18732–18744.
49 D. C. A. S. De Santana, K. Dias, J. G. Souza, A. T. Ogunjimi, M. C. Souza, R. S. Silva and R. F. V. Lopez, *Molecules*, 2017, **22**, 104.
50 A. P. de Sousa, A. F. Fernandes, I. A. Paz, N. R. F. Nascimento, J. Ellena, E. H. S. Sousa, L. G. F. Lopes and A. K. M. Holanda, *J. Braz. Chem. Soc.*, 2017, **28**, 2117–2129.
51 C. D. S. Silva, I. A. Paz, F. D. Abreu, A. P. de Sousa, C. P. Veríssimo, N. R. F. Nascimento, T. F. Paulo, D. Zampieri, M. N. Eberlin, A. C. S. Gondim, L. C. Andrade, I. M. M. Carvalho, E. H. S. Sousa and L. G. F. Lopes, *J. Inorg. Biochem.*, 2018, **182**, 83–91.
52 D. B. G. Mateus, A. P. L. Batista, R. L. Rodrigues and S. Nikolaou, *J. Braz. Chem. Soc.*, 2020, **31**, 2319–2330.
53 M. I. F. Barbosa, G. G. Parra, R. S. Correa, R. N. Sampaio, L. N. Magno, R. C. Silva, A. C. Doriguetto, J. Ellena, N. M. B. Neto, A. A. Batista and P. J. Gonçalvese, *J. Photochem. Photobiol., A*, 2017, **338**, 152–160.
54 R. Kumar, A. Yadav, A. Ratnam, S. Kumar, M. Bala, D. Sur, S. Narang, U. P. Singh, P. K. Mandal and K. Ghosh, *Eur. J. Inorg. Chem.*, 2017, **2017**, 5334–5343.
55 H. Thomsen, N. Marino, S. Conoci, S. Sortino and M. B. Ericson, *Sci. Rep.*, 2018, **8**, 1–8.
56 K. Hishikawa, H. Nakagawa, T. Furuta, K. Fukuhara, H. Tsumoto, T. Suzuki and N. Miyata, *J. Am. Chem. Soc.*, 2009, **131**, 7488–7489.
57 Z. Yuan, X. Yang, Y. Ye, R. Tripathi and B. Wang, *Anal. Chem.*, 2021, **93**, 5317–5326.
58 A. Ismailova, D. Kuter, D. S. Bohle and I. S. Butler, *Bioinorg. Chem. Appl.*, 2018, **2018**, 2018–2041.
59 Y. Zhou, W. Yu, J. Cao and H. Gao, *Biomaterials*, 2020, **255**, 120193.
60 B. Pauwels, C. Boydens, L. Vanden Daele and J. Van de Voorde, *J. Pharm. Pharmacol.*, 2016, **68**, 293–304.
61 N. Levin, J. P. Marcolongo, A. Cadranel and L. D. Slep, *Inorg. Chem.*, 2020, **59**, 12075–12085.
62 A. P. de Sousa, E. M. Carvalho, J. Ellena, E. H. S. Sousa, J. R. de Sousa, L. G. F. Lopes, P. C. Ford and A. K. M. Holanda, *J. Inorg. Biochem.*, 2017, **173**, 144–151.
63 A. P. de Sousa, J. S. do Nascimento, A. P. Ayala, B. P. Bezerra, E. H. S. Sousa, L. G. F. Lopes and A. K. M. Holanda, *Polyhedron*, 2019, **167**, 111–118.
64 I. Chakraborty, S. J. Carrington, G. Roseman and P. K. Mascharak, *Inorg. Chem.*, 2017, **56**, 1534–1545.
65 M. N. Pinto, I. Chakraborty, C. Sandoval and P. K. Mascharak, *J. Controlled Release*, 2017, **264**, 192–202.
66 A. D. H. Mejias, A. Poirot, M. Rmili, N. Leygue, M. Wolff, N. Saffon-Merceron, E. Benoist and S. Fery-Forgues, *Dalton Trans.*, 2021, **50**, 1313–1323.

67 M. D. Turlington, L. Troian-Gautier, R. N. Sampaio, E. E. Beauvilliers and G. J. Meyer, *Inorg. Chem.*, 2018, **57**, 5624–5631.
68 M. D. Turlington, L. Troian-Gautier, R. N. Sampaio, E. E. Beauvilliers and G. J. Meyer, *Inorg. Chem.*, 2019, **58**, 3316–3328.
69 A. C. Roveda, W. G. Santos, M. L. Souza, C. N. Adelson, F. S. Gonçalves, E. E. Castellano, C. Garino, D. W. Franco and D. R. Cardoso, *Dalton Trans.*, 2019, **48**, 10812–10823.
70 H. Yoon, S. Park and M. Lim, *J. Phys. Chem. Lett.*, 2020, **11**, 3198–3202.
71 D. C. Pectol, S. Khan, R. B. Chupik, M. Elsabahy, K. L. Wooley, M. Y. Darensbourg and S.-M. Lim, *Mol. Pharmaceutics*, 2019, **16**, 3178–3187.
72 H. Yoon, S. Park and M. Lim, *ACS Omega*, 2021, **6**, 27158–27169.
73 T. N. Rohrabaugh, K. A. Collins, C. Xue, J. K. White, J. J. Kodanko and C. Turro, *Dalton Trans.*, 2018, **47**, 11851–11858.
74 R. Cabrera, O. Filevich, B. García-Acosta, J. Athilingam, K. J. Bender, K. E. Poskanzer and R. Etchenique, *ACS Chem. Neurosci.*, 2017, **8**, 1036–1042.
75 Y. R. Pérez and R. Etchenique, *Photochem. Photobiol. Sci.*, 2019, **18**, 208–212.
76 V. Ramu, S. Aute, N. Taye, R. Guha, M. G. Walker, D. Mogare, A. Parulekar, J. A. Thomas, S. Chattopadhyay and A. Das, *Dalton Trans.*, 2017, **46**, 6634–6644.
77 Z. Zhao, K. Qiu, J. Liu, X. Hao and J. Wang, *Chem. Commun.*, 2020, **56**, 12542–12545.
78 B. M. Vickerman, C. P. O'Banion, X. Tan and D. S. Lawrence, *ACS Cent. Sci.*, 2020, **7**, 93–103.
79 L. Ma, Q. Zhao, X. Zhang and X. Chen, *Chem. Phys. Lett.*, 2019, **730**, 253–258.
80 A. Notaro, A. Frei, R. Rubbiani, M. Jakubaszek, U. Basu, S. Koch, C. Mari, M. Dotou, O. Blacque, J. Gouyon, F. Bedioui, N. Rotthowe, R. F. Winter, B. Goud, S. Ferrari, M. Tharaud, M. Řezáčová, J. Humajová, P. Tomšík and G. Gasser, *J. Med. Chem.*, 2020, **63**, 5568–5584.
81 W. Tian, C. Wang, D. Li and H. Hou, *Future Med. Chem.*, 2020, **12**, 627–644.
82 S. Siddamurthi, G. Gutti, S. Jana, A. Kumar and S. K. Singh, *Future Med. Chem.*, 2020, **12**, 1037–1069.
83 A. Dey, J. Dana, S. Aute, A. Das and H. N. Ghosh, *Photochem. Photobiol. Sci.*, 2019, **18**, 2430–2441.
84 C. B. Larsen, G. A. Farrow, L. D. Smith, M. V. Appleby, D. Chekulaev, J. A. Weinstein and O. S. Wenger, *Inorg. Chem.*, 2020, **59**, 10430–10438.
85 D. Cullinane, K. S. Gkika, A. Byrne and T. E. Keyes, *J. Inorg. Biochem.*, 2020, **207**, 111032.
86 L. Zeng, D. Sirbu, P. G. Waddell, N. V. Tkachenko, M. R. Probert and A. C. Benniston, *Dalton Trans.*, 2020, **49**, 13243–13252.
87 L. Zeng, D. Sirbu, N. V. Tkachenko and A. C. Benniston, *Dalton Trans.*, 2021, **50**, 7640–7646.
88 C. Zhang, X. Guo, X. Da, Z. Wang, X. Wang and Q. Zhou, *Dalton Trans.*, 2021, **50**, 10845–10852.
89 L. Xie, L. Wang, R. Guan, L. Ji and H. Chao, *J. Inorg. Biochem.*, 2021, **217**, 111380.
90 S. Chakrabortty, B. K. Agrawalla, A. Stumper, N. M. Vegi, S. Fischer, C. Reichardt, M. Kögler, B. Dietzek, M. Feuring-Buske, C. Buske, S. Rau and T. Weil, *J. Am. Chem. Soc.*, 2017, **139**, 2512–2519.

